POAC'15
Trondheim, Norway

Proceedings of the 23rd International Conference on
Port and Ocean Engineering under Arctic Conditions
June 14-18, 2015
Trondheim, Norway

CFD MODELING OF LOCAL SCOUR AROUND A PAIR OF TANDEM CYLINDERS UNDER WAVE CONDITIONS

Nadeem Ahmad[1], Hans Bihs[1], Arun Kamath[1], Øivind A. Arntsen[1]
[1]Norwegian University of Science and Technology, Trondheim, Norway

ABSTRACT

Local scour in a marine environment can lead to the failure of offshore and coastal structures. This is also the case, when marine infrastructure is built in Arctic conditions. The knowledge and understanding of erosion and sediment transport mechanisms and the correct prediction of the local scour magnitude is crucial for the structural design. In a first step towards numerically modeling the complex physics of local scour in an Arctic environment, local scour for wave conditions around a pair of tandem cylinders is modeled in the current paper. The numerical results are compared with experimental data, showing good agreement. A three-dimensional computational fluid dynamics model is used to calculate the detailed flow field and the resulting sediment transport pattern. The location of the free surface is represented using the level set method, which calculates the complex motion of the free surface in a very realistic manner. For the implementation of waves, the CFD code is used as a numerical wave tank. In order to provide an accurate prediction of propagating waves, the convection terms of the Navier-Stokes equations and the level set method are discretized with the 5th-order Weighted Essentially Non-Oscillatory scheme. The pressure is solved on a staggered grid, ensuring tight velocity-pressure coupling. The numerical model employs a Cartesian grid and complex geometries are treated with an immersed boundary method based on ghost cell extrapolation. Sediment transport is implemented through standard bedload and suspended load formulas. The resulting sediment discharges and concentrations are evaluated with the Exner equation, giving the local erosion and deposition pattern for each time step. For the geometric representation of the moveable sediment bed, the level set method is used.

Keywords: Local scour, diffraction effect, Level set method, numerical wave tank and REEF3D.

INTRODUCTION

Offshore structure platforms are generally supported by a group of cylinders. The cylinders are arranged in a way that the structural stability is maintained. Depending on the design, the cylinders may be arranged in tandem arrangement, side by side arrangement and staggered manner. Other than wave forces on the group of the cylinders, local scour is one of the major causes for structural failure. Even the local scour around a single cylinder in the group may result in the failure of the entire structure. Therefore, detailed research work is needed to define local scour under waves.

The flow around a single cylinder can be described as follows: The horseshoe vortices and wake vortices are formed at the upstream and the shadow regions of the cylinder respectively. In addition to this, a steady streaming that is non-uniform oscillatory motion also occurs around the cylinder sides [Sumer and Fredsøe (1997a)]. Local scour is also affected by diffraction effects, which depend on D/L (where D is diameter of cylinder and L is wave length). According to Isaacson (1979) diffraction effect becomes significant, if D/L is larger than 0.2 and an increment in D/L results in an increase in the maximum scour depth. This is also true for the KC number that scour depth increases with KC number [Sumer and Fredsøe (2001)]. Another parameter, which affects the sediment transport, is the Shields number. Shields number depends upon the viscous shear stress, the pressure force, particle weight (particle diameter) and the density of the fluid and the sediment. If the Shields number is much higher than a pre-defined critical value, sediment particles are stirred up and this results in a higher scour rate.

In addition, complex hydrodynamics such as diffraction effects and jet effects are involved when cylinder are arranged in a group (Sumer and Fredsøe, 1997b). Diffraction effect is bending of waves around the cylinder or between the two cylinders. These effects vary with the gap ratio G/D (where G is the gap between two cylinders) and become larger as gap between the cylinders is reduced. Therefore, including the KC number, the diffraction parameter (D/L) and the Shields number, local scour under waves is also a function of the gap between the two cylinders [Sumer and Fredsøe (1997, 2001)]. The configuration of a cylinder group is another parameter that affect local scour to a large extent. For the same KC number, cylinders diameter, the shield parameter and the gap ratio between the two cylinders, maximum scour depth and contours pattern will be completely different for different arrangements. Studies suggest that side by side arrangements develop more scour than tandem arrangements (Sumer and Fredsøe, 1997b).

3D numerical modelling of the local scour under steady flow conditions around the cylinder has been studied by Olsen and Melaaen (1993). Further Olsen and Kjellesvig (1998) extended this study for the same analysis using the k-ε turbulence model. The finite volume method (FVM) is used to discretize the domain and the Reynolds Averaged Navier-Stokes equation and the model is used to calculate the behaviour of the fluid flow. The semi-implicit Method for Pressure-Linked Equations (SIMPLE) is applied to calculate the non-hydrostatic pressure with bed shear stress reduction on sloping beds and a sediment-slide algorithm. The results showed good agreement with the experiment and empirically calculated maximum scour depth values. Later, Roulund *et al.* (2005) carried out a similar study using the k-ω model. Though the results of this model were satisfactory, the prediction of the free surface profile,

which is one of the important aspects for hydraulic structural design, was still a challenge. Among many others, Liu and Garcia (2008) employed a three-dimensional numerical model with free water surface and mesh deformation for local sediment scour using the VOF method. Later, Afzal *et al.* (2014) carried out the three dimensional numerical analysis of pier scour under current and waves. Numerical simulation of sediment transport under waves for the group of cylinder has not yet been investigated. Specifically configurations like tandem, side by side, square arrangement and effect of spacing between the two cylinders are still a challenge.

The current study numerically investigates the effect of the cylinders arrangement on local scour under waves. Two kinds of configuration, namely tandem arrangement and side by side arrangement, are simulated using the REEF3D sediment module. The calculated maximum scour depth is compared with the laboratory measurements. The study also investigates time development of the local scour for the tandem arrangement and side by side arrangement in detail.

NUMERICAL MODEL

REEF3D (Chella *et al.*, 2015) simulates fluid flow using the three-dimensional continuity and the momentum equations (Reynolds Averaged Navier-Stokes equations).

$$\frac{\partial u_i}{\partial x_i} = 0 \tag{1}$$

$$\frac{\partial u_i}{\partial t} + u_j \frac{\partial u_i}{\partial xj} = -\frac{1}{\rho}\frac{\partial p}{\partial x_i} + \frac{\partial}{\partial x_j}(\nu \frac{\partial u_i}{\partial x_j} - \overline{u_i u_j}) + g_i \tag{2}$$

Where u_i the velocity, ρ is the fluid density, ν is the kinematic viscosity, p is the pressure and g is the acceleration due to the gravity. The convective terms of the RANS equations are discretized with the WENO scheme (Jiang and Shu, 1996) as it can handle large gradients right up to the shock very accurately. The Hamilton-Jacobi version of WENO [Jiang and Peng (2000)] scheme is used for the variables of the free surface and turbulence algorithms. For the explicit treatment of the RANS equation, Chorin's Projection method [Chorin (1968)] is used. Eddy viscosity is solved using k-ω model [Wilcox (1994)] with the transport equations for turbulent kinetic energy k and turbulent dissipation rate ω as mentioned below:

$$\frac{\partial k}{\partial t} + u_j \frac{\partial k}{\partial xj} = \frac{\partial}{\partial x_j}[(\nu + \frac{\nu_t}{\sigma k_\omega})\frac{\partial k}{\partial x_j}] + P_k - \beta^* k\omega \tag{3}$$

$$\frac{\partial \omega}{\partial t} + u_j \frac{\partial \omega}{\partial xj} = \frac{\partial}{\partial x_j}[(\nu + \frac{\nu_t}{\sigma_\omega})\frac{\partial \omega}{\partial x_j}] + \alpha \frac{\omega}{k} P_k - \beta\omega^2 \tag{4}$$

To attain higher order accuracy in the time discretization, the third-order Total Variation Diminishing (TVD) Runge-Kutta scheme (Shu and Gottlieb, 1998) is chosen. It involves three intermediate Euler time steps and calculates the next time step by averaging the three intermediate time steps in a consecutive manner to provide a third order accurate solution. The following steps are followed for the time discretization of function.

$$\phi^1 = \phi^n + \frac{2}{3}\Delta t L(\phi^n)$$

$$\phi^2 = \frac{3}{4}\phi^1 + \frac{1}{4}\phi^1 + \frac{2}{3}L(\phi^n)$$

$$\phi^{n+1} = \frac{1}{3}\phi^2 + \frac{2}{3}\phi^2 + \frac{2}{3}L(\phi^n)$$

An adaptive time stepping approach is used such that that time step size are selected to satisfy the CFL criteria depending upon the maximum velocity in the numerical domain. It improves the solution quality and is the best way to optimize computational power.

The level set method, proposed by Osher and Sethian (1988) is used for interface capturing. In this method level set function represent interface between two phases. It is defined as:

$$\phi(\vec{x},t)\begin{cases} > 0 & if\ \vec{x}\ is\ in\ phase\ 1 \\ = 0 & if\ \vec{x}\ is\ at\ the\ interface \\ < 0 & if\ \vec{x}\ is\ in\ phase\ 2 \end{cases}$$

Level set function is smooth across the interface and provides sharp description of free surface and the sediment bed layer. The level set function is moved with external velocity field in the numerical wave tank. The signed distance property of the level set function is lost when interface moves. A Partial differential equation based initialization procedure presented by Peng *et al.* (1999) is then used to restore the signed distance property of the function.

NUMERICAL MODEL FOR THE SEDIMENT TRANSPORT

There are two major modes of sediment transport; the bedload and the suspended sediment transport. The mode in which particle roll over the bed by induced drag forces in the viscous boundary layer near the bed surface, is called bed-load transport. In the other mode the particles are picked up into suspension by the turbulent flow which is called the suspended load transport [Rijn (1984b)]. In the current study bed-load is computed using van Rijn (1984a) formula;

$$q^*_{b,i} = 0; \tau^*_{c,i} \tag{5}$$

$$q^*_{b,i} = 18.74(\tau^* - \tau^*_{c,i})(\tau^{*0.5} - \tau^{*0.5}_{c,i}); \tau > \tau^*_{c,i} \tag{6}$$

$$\tau^*_{c,i} = \frac{\tau_{c,i}}{(\rho_s - \rho)gd_i} \tag{7}$$

Where, $q^*_{b,i}$ is the dimensionless bed load transport rate, $\tau^*_{c,i}$ is dimensionless critical shear stress, τ^* is dimensionless shear stress, τ_c is critical shear stress, g is gravitational acceleration and d_i is particle diameter. Suspended load is calculated using van Rijn formula for the suspended load (Rijn, 1984b). The governing equation for suspended load is a standard convection diffusion equation. The numerical treatment for this transport equation is similar to that of the momentum equations:

$$\frac{\partial c}{\partial t} + u_j \frac{\partial c}{\partial xj} + w_s \frac{\partial c}{\partial z} = \frac{\partial}{\partial x_j}(\Gamma \frac{\partial c}{\partial x_j}) \tag{8}$$

$$c_{bed,susload,i} = 0.015 \frac{d_i}{a} \frac{(\frac{\tau - \tau_{c,i}}{\tau_{c,i}})^{1.5}}{(d_i(\frac{\rho_s / (\rho_w - 1)g}{\nu^2})^{1/3})^{0.3}} \tag{9}$$

Here ρ_s is the density of the sediment, ρ is the density of the water and d_i the sediment particle diameter. Bed level changes are computed by using the Exner formula for the sediment mass balance for the cells closest to bed:

$$(1-n)\frac{\partial z_b}{\partial t} = -\frac{\partial q_{b,x}}{\partial x} - \frac{\partial q_{b,y}}{\partial z} - E + D \tag{10}$$

Where q_b is the bed load, n is porosity, z_b is local bed surface elevation, E is the erosion rate caused due to external actions and D is the corresponding deposition rate that can be defined as:

$$D = w_s c_b \tag{11}$$

$$c_{(bed,susload,i)} = \frac{E}{w_s} \tag{12}$$

Where w_s is fall velocity for the sediment particles.

EXPERIMENTAL SETUP AND NUMERICAL WAVE TANK

The experiments were carried out in a wave flume (28 m long, 4 m wide and 1 m deep) at the Department of Hydrodynamics and Water Resources (ISVA), Technical University of Denmark (Sumer and Fredsøe, 1997b). Different configuration such as tandem, side-by-side, staggered, square group etc., were tested. The diameter of each cylinder is 90 mm and the gap ratio G/d = 0.98 is maintained. The bottom depth of the flume is filled with the fine sediment (d_{50} = 0.2 mm and density = 2650 kg/m^3). The waves of time period T = 4.5 second and maximum wave velocity U_m = 26 cm/s is generated. The flow depth of 0.40 m is maintained. The experiment was run for 1 hour. Maximum scour depth and time development were noted until the equilibrium state was achieved. The tandem and side by arrangement for two cylinders is shown below. Where G is the gap between the two cylinders and d is the diameter of the cylinders.

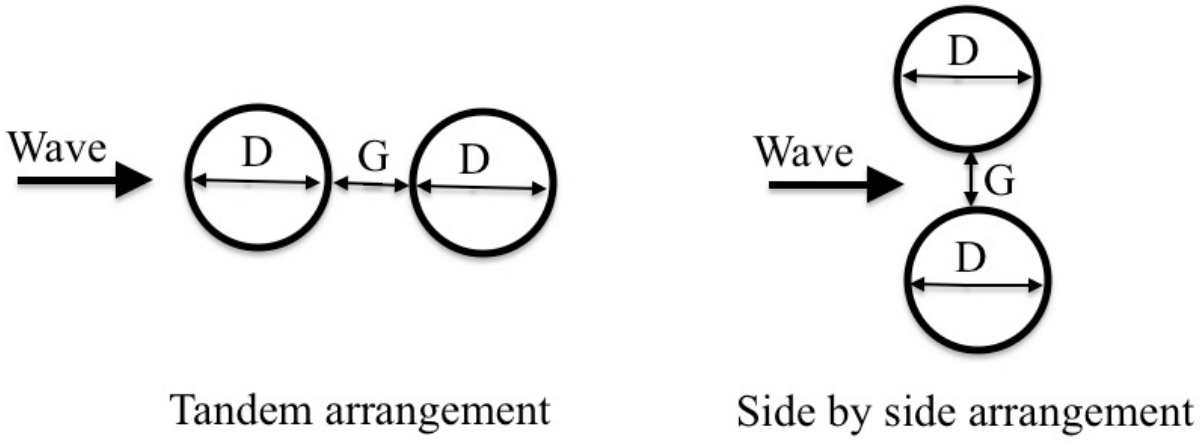

In the numerical study two cylinders with tandem and side by side arrangement are used. The numerical wave tank, 2m long, 1 m wide and 1 m deep with 2 cm cell size is chosen for the wave generation. Two cylinders in tandem and side by side arrangements with a specified gap ratio G/D = 0.98, are placed at centre location of the tank. The first order Cnoidal waves (KC = 13) are generated using the active wave absorption method (Higuera *et al.*, 2013). Waves are generated by providing the elevation and velocities at the wave generation and the beach. In order to avoid reflected waves from the beach, velocity opposite to the reflected waves is prescribed. In this way wave generation and absorption is handled in the numerical wave tank.

RESULTS

The simulated scour depths listed in table 1, showing good agreement with the experimental observation by Sumer and Fredsøe (1997b). Experimental value of the maximum scour for tandem arrangement is 25.20 mm for G/D = 0.98, while the simulated maximum scour depth is 21.60 mm; with a difference of almost 14%. For the side by side arrangement, the simulated scour depth is 36.6 mm with a small difference of 7.5%. The comparison of numerical results with experimental data by Sumer and Fredsøe (1997b) is shown in Table. 1.

Table 1. Test conditions and wave parameter used for numerical simulation (Cylinder diameter, D = 90 mm)

Wave period (sec)	KC	Gap ratio (G/D)	Experimental scour depth (mm)	Simulated scour depth (mm)
Tandem, two cylinders				
4.5	13	0.98	25.2	21.6
Side by side, two cylinders				
4.5	13	0.98	39.6	36.6

The time development of the local scour in the simulation is shown in Figure 1. For both cases, the scour depth increases with the time and attains an equilibrium state in an hour. Time development of scour is recorded every 5.0 s until the equilibrium state is achieved.

Moreover, the time taken to achieve equilibrium state is almost the same but the scour magnitudes are different.

The side by side arrangement is seen to develop a deeper scour than the tandem arrangement. This happens because the side by side arrangement creates a jet effect between the cylinders while tandem arrangement is influenced more by the diffraction effect between the cylinders. In addition, diffraction effect is a function of the gap ratio between the two cylinders and increases when the gap ratio between the two cylinders is reduced. Moreover, local fluctuations in scour depth are also seen in the graph which representing sediment removal and refilling process with wave back and forth action.

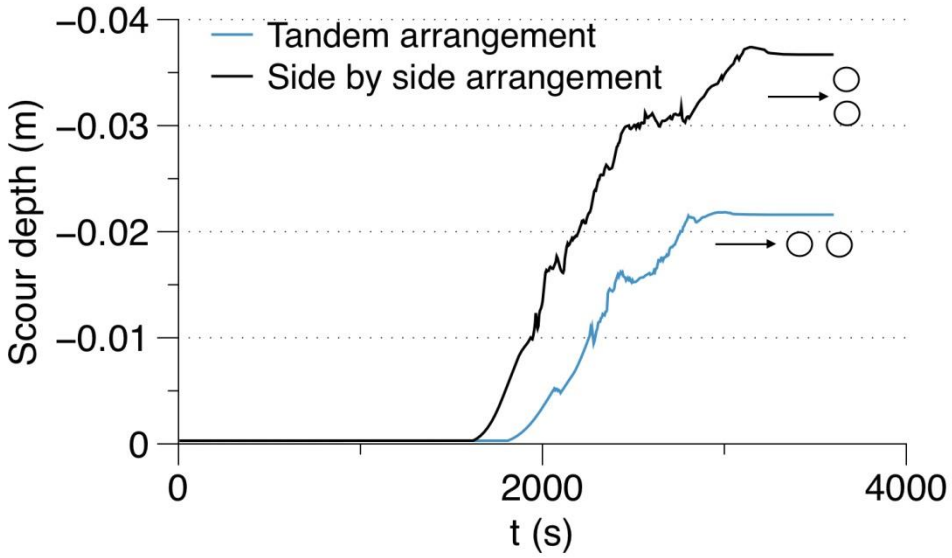

Figure 1. Temporal variation of the local scour for the tandem and side by arrangement

Tandem arrangement

The simulated scour depth is 21.60 mm and the location of the local scour is matches well with the experimental data (Sumer and Fredsøe, 1997b). It is obvious from the Figure 2, that there is no scour in the region between the two cylinders and only small amount of scour is seen around the second cylinder. In addition maximum scour is seen at the upstream side of the first cylinder and maximum deposition around the second cylinder.

Figure 2 shows the 3D scour contours with the water particle velocity at the free surface for the tandem arrangement. Two cylinders are placed along the direction of the wave propagation. The wave is first incident on the upstream side of the first cylinder and it generates high velocity at the upstream edges. The high velocity components develop high bed shear stresses that results in maximum scour at the upstream edges of the cylinder. In addition, the downstream side of the first cylinder is in the shadow region, where the velocities are low. Therefore, all the picked up sediment from the high bed shear stress zone is deposited to the low shear stress zone. Due to the low velocities (low bed shear stresses) in the region between the cylinders and the downstream side of the second cylinder, there is no observed scour. Eventually, the first cylinder (confronting) developed maximum scour and

minimum deposition while second cylinder developed minimum scour and maximum deposition as shown in Figure 2.

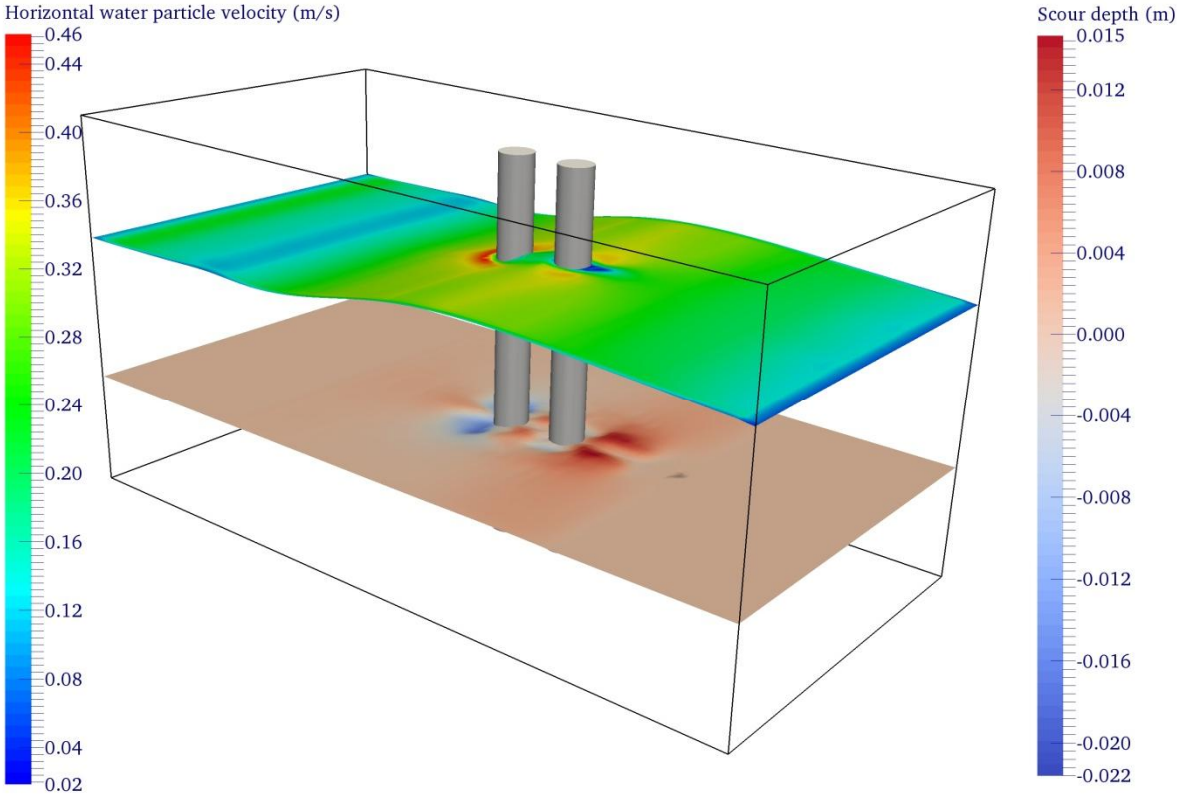

Figure 2. 3D view of scour around the cylinders and free surface velocity for the tandem arrangement

Side by side arrangement

In this arrangement, both the cylinders are directly exposed to the incident waves. As shown in Figure 3, the horizontal water particle velocity between the two cylinders is maximum, which leads to maximum scour in the region. In addition, velocity at the edges of the cylinder is also high, resulting in high scour at the edges as well. On the other hand, velocities at the downstream side are low, resulting in low bed shear stresses. Thus, no scour occurs at the downstream side of the cylinders and all the picked up sediment from the upstream is deposited to the downstream of the cylinders. It is interesting to note that the maximum simulated scour depth is 36.60 mm which is almost 70% higher than in the case of the tandem arrangement. Moreover, almost 85% of the vicinity of the cylinders is surrounded by scour. This can be attributing to the large blocking area, result in high disturbance around the cylinder. In comparison to the tandem case, extent of the scour is also larger. Ultimately, though diameter and the gap ratio are the same for both the arrangements; hydrodynamics, scour pattern and scour magnitude are different for each case.

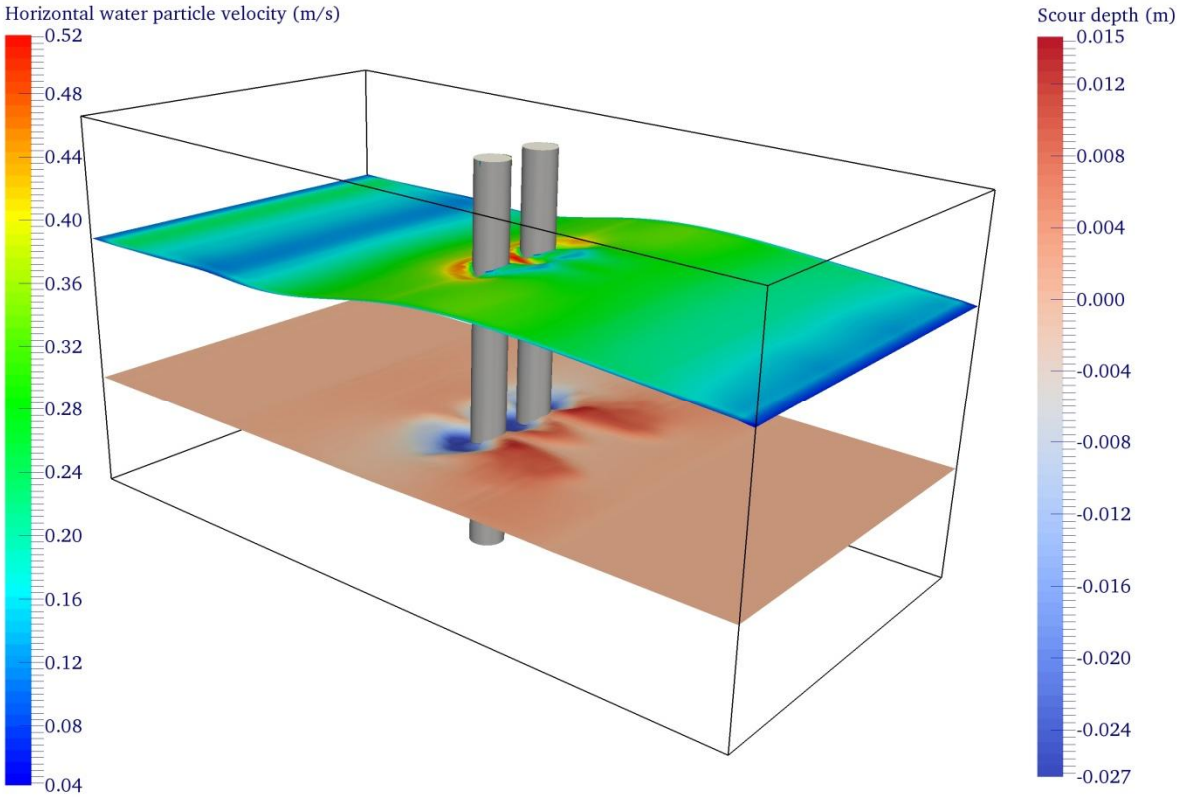

Figure 3. 3D view of scour around the cylinders and free surface velocity for the side by side arrangement

CONCLUSIONS

Numerical simulations of the local scour around tandem cylinders and side by side cylinders arrangement are carried out using the REEF3D. The location of the free surface is calculated with the interface capturing level set method. The model is used as a numerical wave tank. And the first order Cnoidal waves are generated using the active wave absorption method. The calculated scour pattern is compared with laboratory measurements and a good agreement is seen. The following conclusions can be drawn for the simulation performed in this study:

1. Despite the same KC number and gap ratio between the two cylinders, scour is highly affected by arrangements of the cylinder.
2. The tandem arrangement develops 30% lesser scour depth compare to the side by side arrangement.
3. The local scour area domain for the side by side arrangement is much higher than the tandem arrangement and covers almost 85% of cylinder's circumference.

ACKNOKLEDGEMENT

This research leading to these results has received funding from the Polish-Norwegian Research Programme operated by the National Centre for Research and Development under the Norwegian Financial Mechanism 2009-2014 in the frame of Project Contract No. POL-NOR/200336/95/2014

REFERENCES

Afzal, M. A., Bihs, H., Kamath, A. and Arntsen, Ø. A. 2014. Three Dimensional Numerical Modelling of Pier Scour under Current and Waves Using Level Set Method. Proc. 33rd International Conference on Ocean, Offshore and Arctic Engineering, Volume 2: CFD and VIV, San Francisco, USA.

Chella, M. A., Bihs, H., Myrhaug, D. and Muskulus, M. 2015. Breaking Characteristics and Geometric Properties of Spilling Breakers over Slopes. Coastal Engineering, 95, 4-19.

Chorin, A. 1968. Numerical Solution of the Navier-Stokes Equations. Mathematics of Computation, 22, 745-762.

Higuera, P., Lara, L. J. and Losada, I. J. 2013. Realistic Wave Generation and Active Wave Absorption for Navier–Stokes Models Application to Openfoam. Coastal Engineering, 71, 102-118.

Isaacson, M. 1979. Wave Induced Forces in the Diffraction Regime, Pitman Advanced Publishing Program.

Jiang, G. S. and Peng, D. 2000. Weighted Eno Schemes for Hamilton-Jacobi Equations. SIAM Journal on Scientific Computing, 21, 2126-2143.

Jiang, G. S. and Shu, C. W. 1996. Efficient Implementation of Weighted Eno Schemes. Journal of Computational Physics, 126, 202-228.

Liu, X. and Garcia, M. 2008. Three-Dimensional Numerical Model with Free Water Surface and Mesh Deformation for Local Sediment Scour. Journal of Waterway, Port, Coastal and Ocean Engineering, 134, 203-217.

Olsen, N. R. B. and Kjellesvig, H. M. 1998. Three-Dimensional Numerical Flow Modelling for Estimation of Maximum Local Scour Depth. IAHR Journal of Hydraulic Research, 36, 579-590.

Olsen, N. R. B. and Melaaen, M. C. 1993. Three-Dimensional Calculation of Scour around Cylinders. Journal of Hydraulic Engineering, 119, 1048-1054.

Osher, S. and Sethian, J. A. 1988. Fronts Propagating with Curvature- Dependent Speed: Algorithms Based on Hamilton-Jacobi Formulations. Journal of Computational Physics, 79, 12-49.

Peng, D., Merriman, B., Osher, S., Zhao, H. and Kang, M. 1999. A Pde-Based Fast Local Level Set Method. Journal of Computational Physics, 155, 410-438.

Rijn, L. C. V. 1984a. Sediment Transport, Part I: Bed Load Transport. Journal of Hydraulic Engineering, 110, 1431-1457.

Rijn, L. C. V. 1984b. Sediment Transport, Part Ii: Suspended Load Transport. Journal of Hydraulic Engineering, 110, 1613-1641.

Roulund, A., Sumer, B. M., Fredsøe, J. and Michelsen, J. 2005. Numerical and Experimental Investigation of Flow and Scour around a Circular Pier. Journal of Fluid Mechanics, 534, 351-401.

Shu, C. W. and Gottlieb, S. 1998. Total Variation Diminishing Runge- Kutta Schemes. Mathematics of Computation, 67, 73-85.

Sumer, B. M. and Fredsøe, J. 1997a. Hydrodynamics around Cylindrical Structures, World Scientific.

Sumer, B. M. and Fredsøe, J. 1997b. Wave Scour around Group of Verticle Piles. Journal of Waterway, Port, Coastal and Ocean Engineering, 124.

Wilcox, D. C. 1994. Turbulence Modeling for Cfd, DCW Industries Inc., La Canada, California.